

A Full-Scale Simulation and Analysis of Formation Flight during In-Air-Capturing

Sunayna Singh^{a*}, Sven Stappert^a, Leonid Bussler^a, Martin Sippel^a,
Yakut Cansev Kucukosman^b, Sophia Buckingham^b

^a DLR Institut für Raumfahrtssysteme, Linzer Straße 1, 28359, Bremen, Germany, sunayna.singh@dlr.de

^b von Karman Institute for Fluid Dynamics VKI, 72 Chaussée de Waterloo, Rhode-St-Genèse B-1640, Belgium, sophia.buckingham@vki.ac.be

* Corresponding Author

Abstract

In the past two decades, the renewed interest in sustainable space transportation has fueled the development of many innovative reusable launch technologies. One such concept called ‘In-Air-Capturing (IAC)’ involves winged rocket stages captured mid-air and towed back to the launch site using an aircraft. The approach patented by German Aerospace Center (DLR), shows potential for substantial mass and cost reduction by eliminating the need for additional propulsion during the descent. A critical aspect of IAC requires the two involved vehicles to be in a formation flight with similar velocities, altitudes and flight path angles separated by a safe distance. The preliminary requirement is to maintain the formation for a minimum of 60 s, despite any external disturbances.

This paper presents the modelling and simulation of a full-scale reusable launch vehicle and a towing aircraft attempting the formation flight for IAC. First, a suitable aircraft configuration is selected based on the aerodynamic performance of the selected test rocket stage. Important subsystems are also identified and modelled comprehensively. Then, trajectory simulations are performed to identify the best approach and initial conditions for the formation. Sensitivity of the formation flight to several factors like the idle thrust, wake turbulence and wind gusts are also analysed. The simulation yielded that the minimum duration of formation flight could be maintained, despite the external disturbances. Lastly, potential improvements and future simulations are discussed.

Keywords: FALCon, In-Air-Capturing, Reusable Launch Vehicle, Vertical Launch Horizontal Landing.

Acronyms/Abbreviations

3STO	Three Stage To Orbit
AoA	Angle of Attack
CoG	Centre of Gravity
CFD	Computational Fluid Dynamics
DLR	German Aerospace Center
DRL	Down Range Landing
ELV	Expendable Launch Vehicle
FPA	Flight Path Angle
GLOW	Gross Lift-Off Weight
GTO	Geostationary Transfer Orbit
IAC	In-Air-Capturing
L/D	Lift-to-Drag
LFBB	Liquid Fly Back Boosters
LH2	Liquid Hydrogen
LOX	Liquid Oxygen
MECO	Main Engine Cut Off
RANS	Reynolds-Averaged Naviers Stokes
RLV	Reusable Launch Vehicle
RP-1	Rocket Propellant-1 (Kerosene)
RTLS	Return To Launch Site
TA	Towing Aircraft
THS	Trimmable Horizontal Stabilizers
TSTO	Two Stage To Orbit
VTVL	Vertical Take-Off Vertical Landing
VTHL	Vertical Take-Off Horizontal Landing

1. Introduction

In the recent years, the successful development and operation of multiple reusable launch systems has been perceived to be a vital accessory to reduction of launch costs and increase in launch frequencies. The reusable launch systems can be categorised into two types - Vertical Take-Off Vertical Landing (VTVL) and Vertical Take-Off Horizontal Landing (VTHL). Pioneering companies like SpaceX and Blue Origin use VTVL based Reusable Launch Vehicles (RLVs). However, both the currently employed VTVL techniques, namely Return To Launch Site (RTLS) and Down Range Landing (DRL) require significant amount of fuel during descent.

Additionally, VTHL based winged RLVs can only glide back when sufficient energy is available [1]. For larger launchers, this would require descent from an orbit. Moreover, Liquid Fly Back Boosters (LFBB), which is a VTHL system powered by turbofans, also requires an additional propulsion system, adding to its inert mass. In view of these challenges, an innovative approach called ‘In-Air-Capturing (IAC)’ was proposed and patented by DLR [2]. In this approach, a winged-rocket stage is captured mid-air using an aircraft and towed back to the launch site for horizontal landing.

1.1 Performance impact

Any RLV mode of operation tends to degrade the launcher’s performance compared to an Expendable Launch Vehicle (ELV) due to the added stage inert mass or required descent propellant. However, amount of performance degradation varies over a significant range depending on the mode of operation or separation conditions. Although a precise estimation of RLV costs is unattainable, the performance impact can provide a sound indication of the potential of different RLV modes.

The performance impact of a RLV can be directly related to its ascent inert mass ratio or net-mass fraction, reasonably assuming that the engine specific impulse is not considerably affected. Inert mass of the stage ($m_{i,inert}$) during ascent flight consists of its dry mass and its total residual propellants including the propellant needed for controlled re-entry, landing or possible fly-back. The inert mass ratio (ζ_i) can then be defined as:

$$\zeta_i = \frac{m_{i,inert}}{m_0} \quad (1)$$

Where m_0 stands for Gross Lift-Off Weight (GLOW) of the RLV stage. Therefore, higher the inert mass ratio of a stage, lower would be its acceleration performance when the propellant type and engine performance are kept constant. Fig. 1 presents a comparison of the inert mass ratio for generic Two Stage To Orbit (TSTO) launchers using different return modes of the reusable first stage. All launchers have been sized for a Geostationary Transfer Orbit (GTO) payload of 7.5 tons. They are analysed with different types of propellants (LOX-LH2, RP-1, LOX-CH4) as well as different propellant loading. As the mission and number of stages are identical, the inert mass ratio can be represented as a function of total ascent propellant loading.

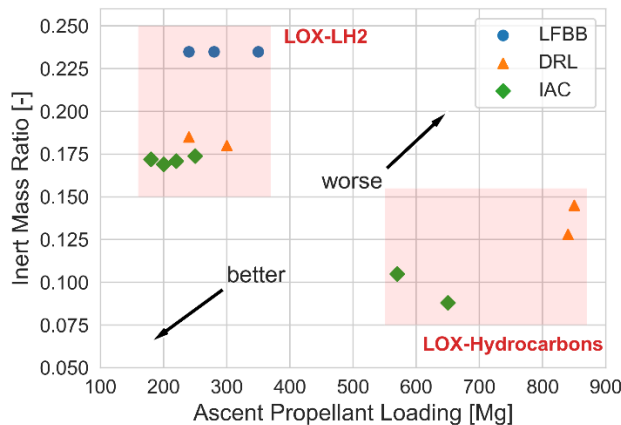


Fig. 1. Performance Impact of Different Return Modes

It can be observed from Fig. 1 that the IAC mode provides the lowest inert masses across different propellant types when compared to LFBB mode, which requires a turbojet to fly back and the DRL, which requires propellant to land. The corresponding ascent propellant required for the mission is also smaller with IAC. A detailed comparative study of different RLV modes can be found in [3]. Therefore, IAC has a high potential for both mass and cost reduction and should be examined in further detail. It must also be mentioned that the application can not only be used for partial or complete recovery of launch vehicles but also for smaller parts like fairings.

1.2 Horizon 2020 Project FALCon

To facilitate the development of IAC technology, a Horizon 2020 project named FALCon (**F**ormation flight for in-Air Launcher 1st stage **C**apturing demonstration) has been kicked-off on March 2019. With a total funding of 2.6 M€, the FALCon project aims to address three key topics:

- IAC Development Roadmap and Economic Benefit Assessment.
- IAC Experimental Flight Demonstration
- IAC Subscale and Full-Scale Simulations

The project involves international cooperation of seven European partners (mentioned in Table 1) led by DLR. The current paper will address a part of the full-scale simulations performed in the scope of the FALCon project. Furthermore, with the laboratory scale flight demonstration of two fully autonomous test vehicles (which are currently in preparation), the EC funded project intends to bring the TRL level of IAC-recovery method to beyond 4 by 2022.

Table 1. List of FALCon Project Partners

Participating Organisation Name	Country
1 German Aerospace Center (DLR)	Germany
2 von Karman Institute for Fluid Dynamics (VKI)	Belgium
3 Drone Rescue Systems GmbH	Austria
4 Soft2Tec GmbH	Germany
5 Astos Solutions SRL (ASTOS)	Romania
6 Institute of Mechanics, Bulgarian Academy of Sciences (IMEch-BAS)	Bulgaria
7 Embention	Spain

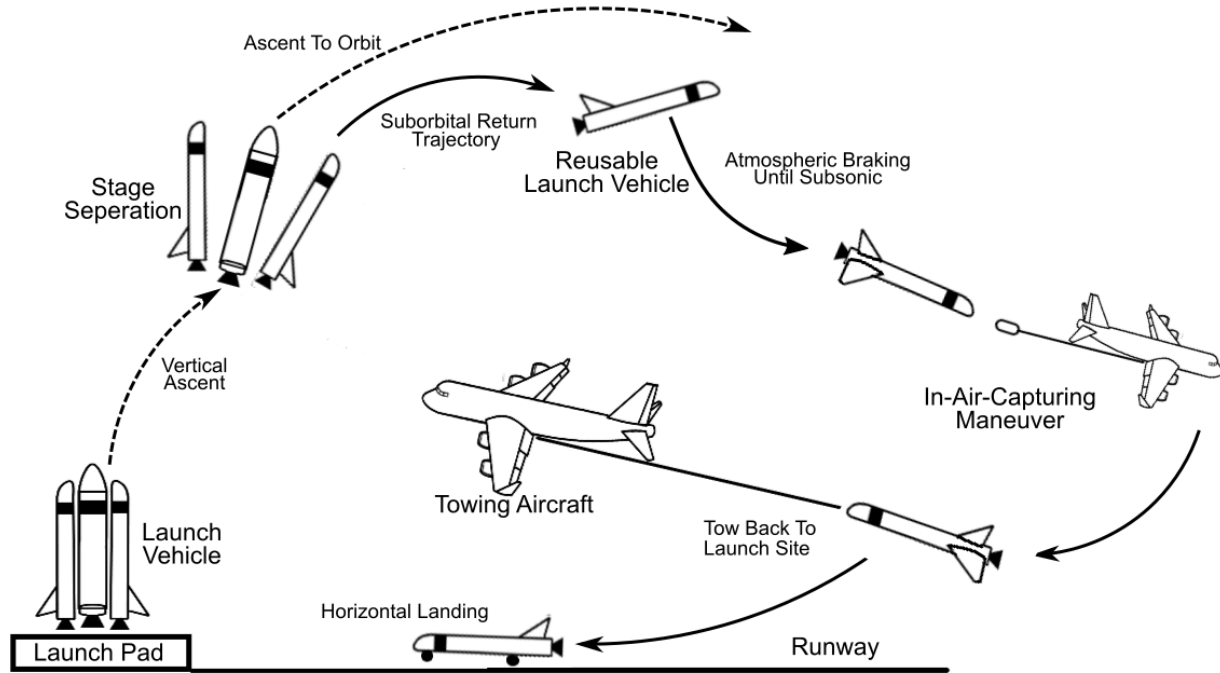


Fig. 2: Complete Mission Cycle of IAC

1.3 Mission Profile

Fig. 2 shows the complete mission cycle of IAC. The process starts with a vertical launch from the launch pad. At Main Engine Cut Off (MECO), the winged first stage separates from the launch vehicle and the second stage moves on to the orbit. The first stage then begins a ballistic re-entry such that its velocity is reduced from supersonic to subsonic through atmospheric braking. In the meantime, a Towing Aircraft (TA) loiters at approximately 10 km altitude until the RLV is in the vicinity. Then, between an altitude of 2 km and 8 km, the TA approaches the RLV to form a gliding parallel formation. During this manoeuvre, a capturing device is released from the TA, which autonomously ensures mating of the two bodies. Finally, the RLV is towed back to an airstrip where it lands horizontally [4].

This paper examines the first sector of the IAC mission profile called the formation flight phase using full-scale (or large scale) test cases. To achieve a parallel formation, the altitude, velocity and Flight Path Angle (FPA) of the RLV and TA have to be comparable. This would require close consideration of the aerodynamic configuration of the two vehicles. Therefore, in Sec. 2 the test cases are introduced and their aerodynamic performance is analysed using empirical methods for the selection of the most suitable configurations. Then, to get a more sensible model for the formation trajectory simulations, important subsystems are analysed in Sec. 3. This includes aerodynamic modelling of selected configurations and aircraft wake using high fidelity

methods, analysis of system mass and its effects on aerodynamics, and modelling of the aircraft propulsion system. This is followed by results in Sec. 4, wherein the formation flight simulations are presented. Sensitivity to several factors like idle thrust, initial conditions and external disturbances are also examined here. The end goal is to maintain at least 60 s of formation despite external disturbances for the capturing device to establish contact with the RLV. Finally, the paper is concluded in Sec. 5, and the future work is presented.

2. Selected Configurations for Formation Flight

The parallel formation for IAC requires both the participating vehicles to be in a gliding flight with similar altitudes, velocities and FPAs separated by a safe distance. One critical aspect to ensure such a formation is that the aerodynamic performance of both the RLV and TA should be closely matched.

Typical winged re-entry vehicles have a maximum Lift to Drag (L/D) ratio between 2-4.5 in subsonic regime, as documented by Saltzman [5]. On the other hand, long range commercial aircraft can reach a L/D ratio of up to 20 [6]. Therefore, to reduce this gap in aerodynamic performance and prepare the vehicles for a successful formation, careful design selection and alterations may be required. In the coming section, the chosen full-scale test cases are presented. The modifications that may be required for the formation flight are also identified and presented.

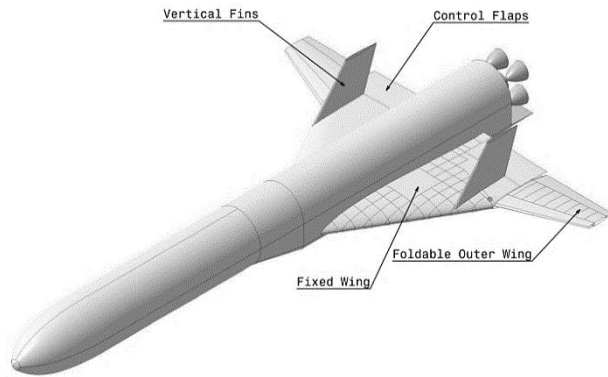


Fig. 3: Subsonic Configuration of RLVC4 [7]



Fig. 4: Commercial Airliner: A340-600 [8]

1.4 Reusable Launch Vehicle (RLV)

For the current research, the RLV is selected to be the first stage of a 3 Stage-To-Orbit (3STO) launch vehicle proposed in [7]. This returning winged stage called RLVC4-IIIB has a special swept wing configuration. The outer wings of the spacecraft are folded in during the hypersonic re-entry to avoid shock-shock interaction [9]. Then, once the vehicle has slowed down to subsonic velocity, the outer wings are deployed (or unfolded) as shown in Fig. 3. The larger wings facilitate a higher trimmed L/D ratio of up to 5.5 in the subsonic regime, making the configuration advantageous for IAC. The configuration uses control flaps for trimming and maneuvering, which can deflect up to $\pm 20^\circ$. Some additional characteristics of the RLV are presented in Table 2. Other variants of the RLV can also be used for IAC are given in [10].

Table 2. Characteristics of RLVC4 [7]

Property	Value
Dry Mass [kg]	69,670
Ascent Propellant [kg]	340,000
Gross Lift-Off Mass [kg]	417,800
Mass during descent [kg]	79,182.6
Total Length [m]	59.5
Fuselage Width [m]	5.4
Wing Span (deployed) [m]	35.5

1.5 Towing Aircraft (TA)

Based on the scale of the RLV, a suitably sized TA must be selected. For the current application of capturing a large 80-tonne RLV, an Airbus A340-600 (shown in Fig. 4) is considered fit [3]. The long-range jetliner with large loading capacity and four powerful Rolls Royce Trent 556 engines can support the towing loads from the large stage. The relatively advanced flight control system is also advantageous for the complex manoeuvres required in IAC. Further, repurposing the retired fleet would not only prove to be economically advantageous but also add a component of reusability to the now withdrawn aircraft. Some basic aircraft characteristics are summarised in Table 3.

Table 3. Characteristics of A340-600 below [11]

Property	Value
Maximum Take-Off Weight [kg]	365,000
Maximum Landing Weight [kg]	265,000
Maximum Zero-Fuel Weight [kg]	251,000
Maximum Payload [kg]	68,000
Total Length [m]	75.24
Fuselage Width [m]	5.64
Wing Span without Winglet [m]	61.20

The cruise L/D ratio for a typical aircraft from the A340 family can reach up to 19.3 [6]. However, for the capture of RLVC4-IIIB using IAC, the desired L/D ratio is close to 5.5. Therefore, some additional drag sources must be included to lower the L/D ratio of the TA. Drag can be generated using the existing control surfaces like the spoilers and also, other components such as landing gear.

According to the Airbus Maintenance manual [11], an A340-600 consists of three sets of landing gear:

- Two main landing gears with four-wheel assembly that are located under the wing and retract sideways towards the fuselage.
- A centreline landing gear with four wheels that is located at the belly of the aircraft and retract forward.
- A nose landing gear with twin wheels that retracts forward below the cockpit.

Additionally, the spoilers can be deflected up to -30° for the speed brake function. However, to consider some room for manoeuvrability, deflection of only up to -20° is considered. To find the configuration with the closest L/D ratio to the chosen RLV, different TA configurations were analysed using empirically generated aerodynamic datasets as presented in Table 4.

From Table 4, two potential configurations (TA4 and TA5) provide a close match to the target L/D of 5.5. However, TA4 required lesser components, which would reduce any structural and wake associated disturbances originating from the landing gear deployed mid-air.

Further, the centreline landing gear can be removed to house the capturing device in the bay and provides close access to the structural elements near the aircraft Center of Gravity (CoG) for the distribution of towing loads. Therefore, TA4 is selected to be the most suited configuration and its aerodynamics is further analysed using high fidelity Computation Fluid Dynamics (CFD).

Table 4. Analysis of Aerodynamic Performance for Different TA Configurations using Empirical Methods

Description	L/D ratio
TA1 Clean Configuration	19.36
TA2 Spoilers -20°	12.97
TA3 Front Landing Gear Deployed, Spoilers -20°	10.02
TA4 Front and Main Landing Gear Deployed, Spoilers -20°	6.25
TA5 All Landing Gears Deployed, Spoilers at -20°	4.78

3. Modelling and Analysis of Subsystems

For a realistic simulation of the full-scale scenario of IAC, some important subsystems must be reliably modelled. The trajectory not only depends on the aerodynamics of the vehicles, but also mass configuration, propulsion and external disturbances like wake from the TA. In the coming section, modelling of these crucial aspects are presented and their potential effects on the formation trajectories are analysed.

3.1 Aerodynamics

RLVC4-IIIB and A340-600 were selected in Sec. 2 as the suitable test cases for IAC. The aerodynamics of these configurations are analysed using Reynolds-Averaged Naviers Stokes (RANS) to achieve high confidence datasets. The CFD simulations are performed using the open source code OpenFOAM v6.0. Both vehicles are analysed at the flight point shown in Table 5. Since the flight point exists in the compressible subsonic flow regime, the rhoSimpleFoam solver is selected. Several turbulence models are tested on a simplified model (NACA 0012 airfoil) with the same regime to find the most suited model for the respective flow type. The analysis found k- ω SST turbulence model to be the most accurate for predicting flow areas [12]. A sensitivity study on mesh density is also performed to assure a computationally effective yet accurate grid resolution.

Table 5. Simulation Flight Point for RANS [12]

Parameter	Value
Velocity [m/s]	142.39
Mach	0.45
Altitude [m]	6000
Pressure [Pa]	47248.92
Density [kg/m ³]	0.66065

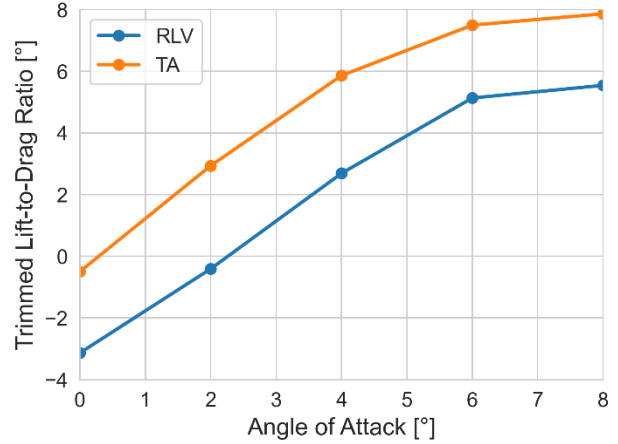


Fig. 5. Aerodynamic Performance of RLV and TA using CFD Dataset

Fig. 5 shows the comparison of aerodynamic performance obtained using RANS simulations. It can be observed that the selected TA configuration with spoilers deployed at -20°, and with front and main landing gears deployed can reach a trimmed L/D ratio of 8, while the RLV only reaches a trimmed L/D ratio of 5.5 at an Angle of Attack (AoA) of 8°. Although the performance is not identical, yet they may be similar enough to maintain a formation of up to 60 s required for the IAC capture phase. The final formation trajectories using these aerodynamic datasets will be analysed in the results.

3.2 System Mass

The current large-scale scenario involves two sizable aircraft. The RLV descending with an unpowered glide is assumed to have a constant mass throughout the formation flight of about 80 tons. For the TA, the dive configuration is considered to have no payload and some additional parts like the central landing gear removed. With this, the aircraft is expected to weigh between 180 tons to 310 tons for formation flight depending on the required trip fuel. However, the mass of the aircraft also affects its aerodynamic behaviour. This effect can be observed with a sensitivity study performed using the basic 3DOF steady flight equations of motion given as follows:

$$m\dot{V} = T + W \sin \gamma - D \quad (2)$$

$$mV\dot{\gamma} = L - W \cos \gamma \quad (3)$$

Here, V is the velocity in m/s, m is the mass of the aircraft in kg, L is the lift force, D is the drag force, T is the thrust, W is the weight of the aircraft and γ is the FPA in radians. For the study, it was assumed that the velocity and FPA of the system remains constant and the thrust acts only in the direction of velocity. The results of this sensitivity study are shown in Fig. 6.

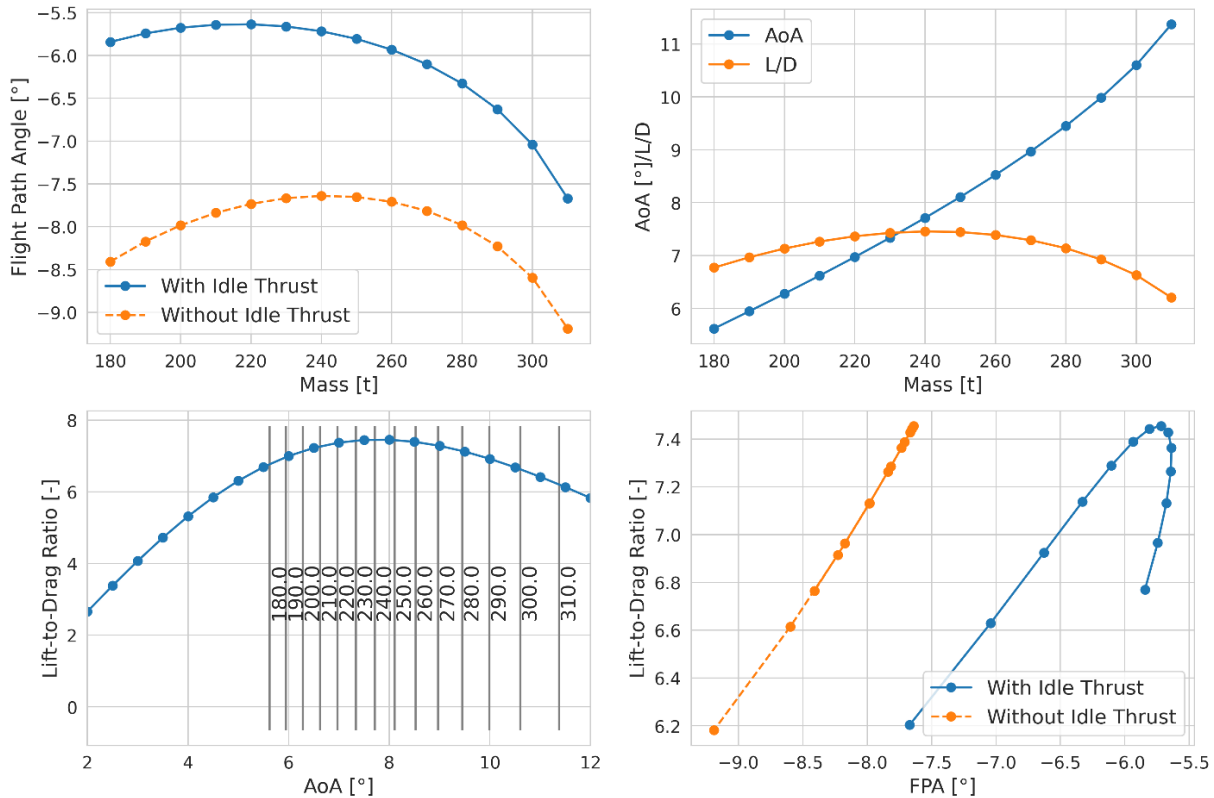


Fig. 6. Sensitivity of TA Aerodynamics to Mass and Idle Thrust

Fig. 6 shows the relationship between aerodynamic angles, L/D ratio and mass. The effect of idle thrust is also included, which will be discussed in the next section. It can be observed that the larger the TA mass, the higher the AoA it can achieve. Further, the L/D ratio is also reduced (compared to its maximum) with larger masses. Since a large AoA (up to 10°) can help slow down the aircraft during descent, a heavier configuration seems favourable. Also, a lower FPA may be required due to the RLV descending steeply (low L/D ratio). Based on these factors, a mass of 280 tons was selected to facilitate a longer formation time.

3.3 Propulsion

The propulsion system for TA is crucial for IAC. For the current test scenario, the A340-600 consists of four powerful Rolls Royce Trent 556 engines. These high-bypass turbofan engines provide a maximum take-off thrust of 260 kN and a maximum continuous thrust of 197 kN each [13]. For the formation flight, the TA needs to be in a gliding descent. Typically for commercial descents, the engines are not completely turned off and kept in idle mode (the minimum throttle setting). For a jet engine, the flight idle RPM varies between 45% to 60%, depending on the manufacturers design [14]. Based on Fig. 7, it can be seen that the corresponding idle throttle value would be between 10% to 20%. Therefore, for the current study, a throttle value of 10% is assumed as idle.

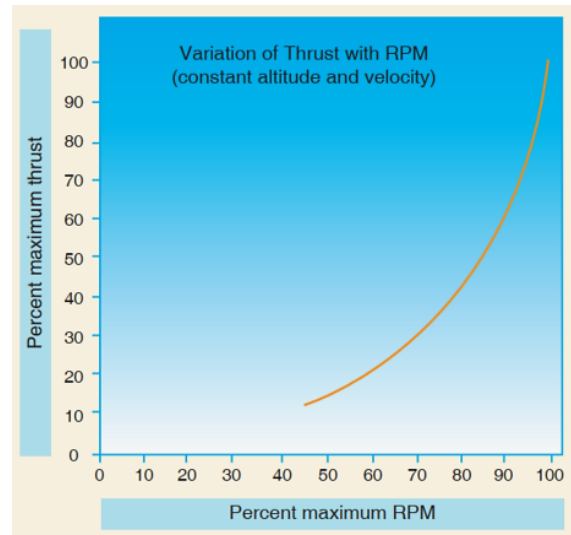


Fig. 7. Variation of Thrust with RPM [14]

Since idle thrust acts against the drag, it would lead to a different aerodynamic performance than original expected using the RANS datasets. This could further increase the gap between TA and RLV L/D ratio and make formation flight more challenging. The effect of idle thrust on aerodynamic angles can be seen in Fig. 6, wherein the achievable FPAs with idle thrust are much larger than the FPAs without idle thrust. Thus, to ensure

longer formation time, it is worthwhile to examine the trajectories without idle thrust. Therefore, the formation flight trajectories will also be examined for sensitivity to idle thrust.

It must be stated that idle thrust is mainly used in commercial airliners for the safety of passengers. Since the engine cannot be throttled up quickly in case a sudden manoeuvre is required, the aircraft being on idle provides more resilience to the pilot. Additionally, turning off engines can increase the drag substantially, which may increase the risk of stall. However, it is possible to shut down and restart the engines mid-flight, as long as the flight is within the operating envelope [15]. Some operating conditions for Rolls Royce Trent 500 series are specified in [13]. Lastly, the formation flight will be attempted within an AoA of 10°, to limit the risk of stall when the flight is unpowered.

Another aspect that cannot be overlooked while modelling the propulsion is that the thrust for airbreathing engines varies with air density. For any fixed throttle setting, the thrust produced at lower altitudes is higher than thrust produced at higher altitudes. This is because the air density is higher close to the Earth. The relationship is included in the model using a basic formula [16]:

$$T = T_{SLmax} \delta_T \left(\frac{\rho}{\rho_{SL}} \right) \quad (4)$$

Where T_{SLmax} is the maximum thrust at sea level in N, δ_T is the throttle setting of the engine, ρ is the air density at the current altitude in kg/m³ and ρ_{SL} is the air density at the sea level in kg/m³.

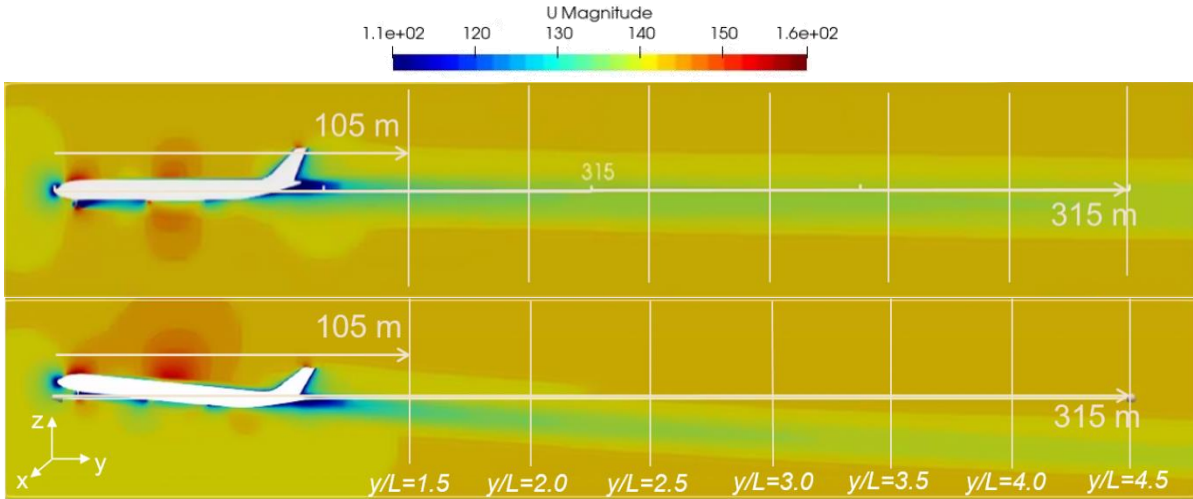


Fig. 8. Wake Velocity Magnitude Contours for AoA of 0° (top) and 6° (bottom) [12]

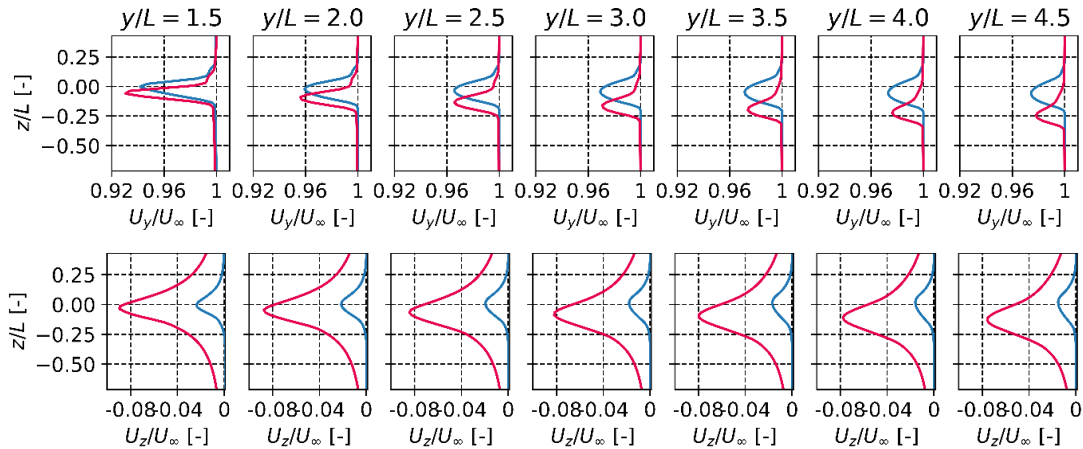


Fig. 9. Wake Profiles in the Fuselage Plane for 0° (blue) and 6° (red) AoA; Streamwise Velocity Component (top) and Downwash Velocity Component (bottom) [12]

3.4 Aircraft Wake

The formation flight requires the RLV to be in close proximity behind the TA (about 350 m for the current test scenario). This means that the aircraft wake can act as a disturbance to the RLV and may lead to loss of formation. The landing gear itself could cause some turbulent flow behavior and add to the disturbance due to wake. Therefore, RANS calculations for the wake were performed for A340-600 with the spoilers at -20° and the front and main landing gears deployed. The same simulation parameters given in Sec. 3.1 were used for the wake. A detailed description of the CFD study of the wake can be found in [12].

Fig. 8 shows the velocity contour plots, wherein the effects of wake can be seen as far as 315 m from the nose of the aircraft. The wake behaviour is also varied with AoA and the effects can be observed more distinctly in Fig. 9. The figure shows the wake velocity components in streamwise direction (horizontal) and downwash direction (vertical) as a function of distance from the aircraft. While the magnitude of the streamwise velocity (U_V) for both 0° and 6° AoA remain similar, a drift in the Z-direction can be observed for 6° AoA. Then, it appears that the magnitude of downwash component (U_Z) is strongly affected by the AoA of 6° . This is evident by the fact that even after moving away from the TA, the downwash velocity component remains close to 8% of the free stream velocity (U_∞). The deficit in velocity caused by this component can possibly affect the AoA of the RLV leading to a disturbance in formation. Thus, it is critical to analyse the sensitivity of the formation flight trajectory to the wake disturbances.

4. Results

An elaborate model is compiled using the subsystems stated in Sec. 3, and linked with environment models like atmosphere, gravity and wind. A simple PID controller is included to influence the velocity, altitude and FPA of both TA and RLV to match a reference trajectory for the RLV. The RLV is controlled and trimmed using flaps that can be deflected up to $\pm 20^\circ$. The TA is trimmed using Trimmable Horizontal Stabilizers (THS), which can be deflected between -14° and $+2^\circ$, and the elevons or elevators that can be deflected between -30° to $+15^\circ$ are used for rapid manoeuvring.

To get a better understanding of the formation flight phase, sensitivity of the trajectory to several factors like idle thrust, initial conditions and external disturbances like wake and wind gusts are analysed. The goal is to maintain a minimum of 60 s of formation to allow the capturing device to attempt the capture of RLV. The criteria or constraints for formation are defined as follows:

- The formation flight must be achieved between an altitude of 3000 m and 8000 m.
- The RLV should remain behind the TA throughout the formation.
- The relative distance between the TA and RLV should be maintained between 70 m to 350 m.
- The relative velocity between the TA and RLV should not exceed ± 3.5 m/s.
- The FPA should be in close agreement.
- The control surfaces should be unsaturated to allow room for manoeuvrability.

The vehicles are considered to be in formation when all the stated criteria are met.

1.1 Sensitivity to Idle Thrust

As it was addressed in Sec. 3.3, jet engines for commercial airliners are typically kept in idle mode for gliding. The idle thrust acting against the drag contributes to the aerodynamic performance of TA, thereby virtually increasing the originally observed L/D ratio. For the formation flight, this could increase the challenges because the gap in the aerodynamic performance of both vehicles is increased. To analyse the impact of this factor, the formation trajectories are analysed both with and without the idle thrust (10% engine throttle).

Fig. 10 shows the formation flight trajectories with and without the idle thrust respectively. It can be observed in Fig. 10(a) that the TA is able to meet the formation criteria for barely 50 s (shaded in green). The main challenge comes from the TA not being able to descend steep enough to match the RLV trajectory. Also, in the lower altitudes, the increased air density leads to increased thrust in TA, which makes the velocities difficult to match. On the other hand, Fig. 10(b) shows that without any thrust, the TA can match the RLV trajectory for a longer duration of approximately 72 s. The TA can now glide at a steeper FPA, allowing it to match the altitude more closely. Moreover, the additional drag helps the TA achieve a closer velocity to the RLV. Lastly, it must also be mentioned that for both the formation trajectories, the control surfaces of the TA and the RLV remained unsaturated as shown in Fig. 11. This means that there is still scope of manoeuvrability, but the formation flight is mainly constrained by the aerodynamic performance.

To conclude, when the idle thrust is considered the TA could not achieve at least 60 s of formation flight required for the capture phase. However, when no idle thrust was included, longer formations of more than 60 s could be maintained. Thus, the latter can be considered the more favourable option and is further analysed.

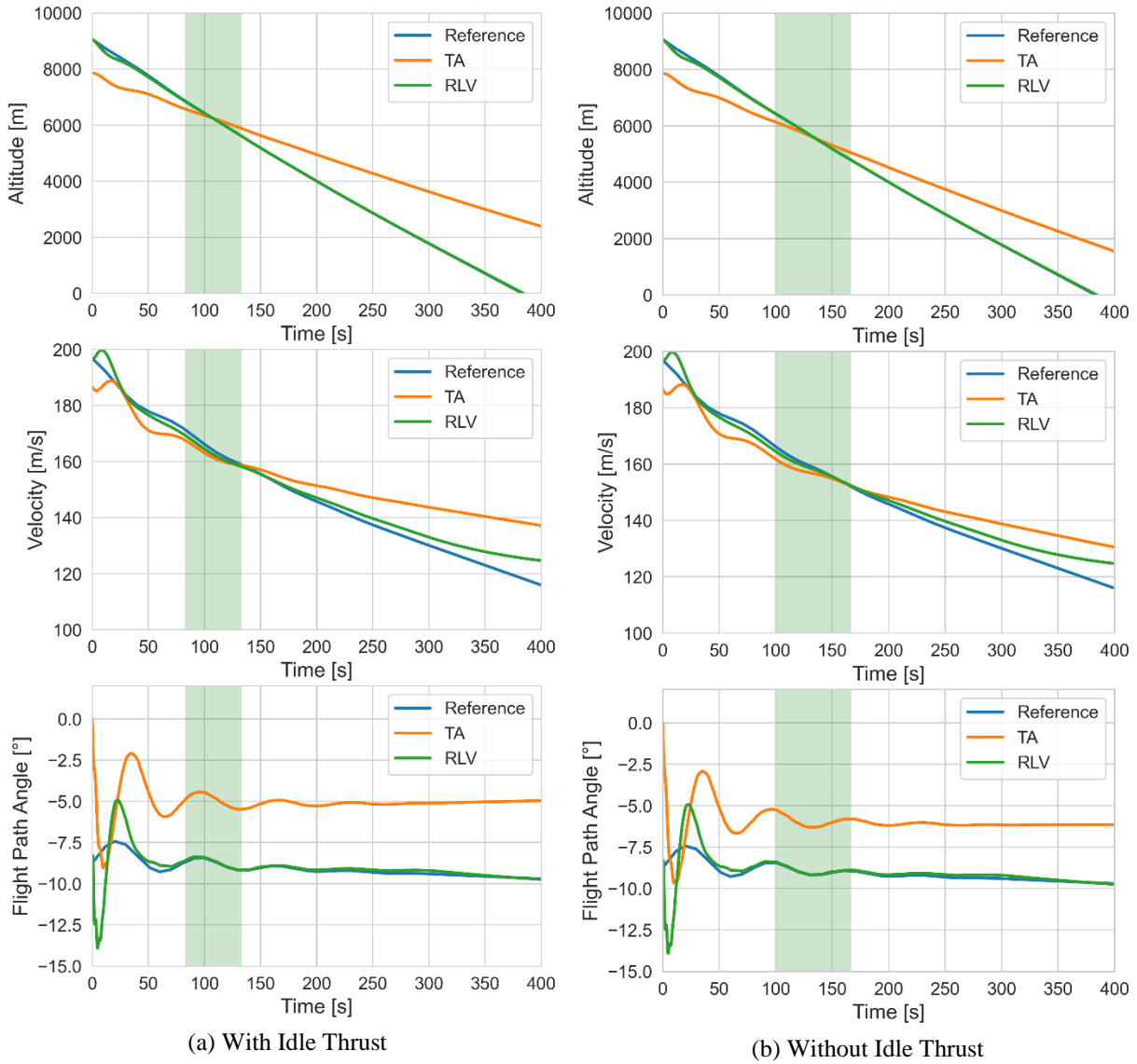


Fig. 10. Formation Flight Trajectory with Idle Thrust (Left) and without Idle Thrust (Right)

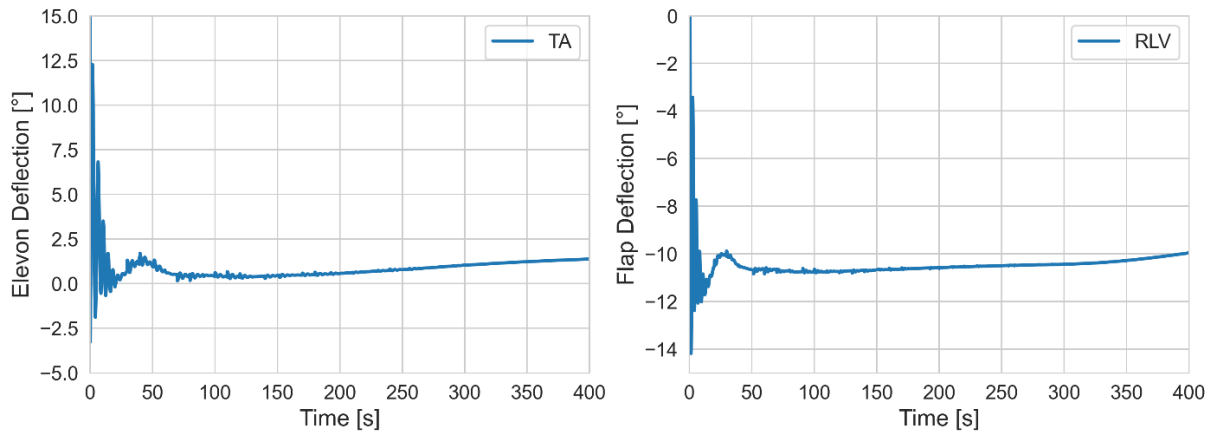


Fig. 11. Control Deflections during the Formation Flight: TA (Left) and RLV (Right)

1.2 Sensitivity to Initial Conditions

Before the formation flight, the TA is cruising and waiting at about 10 km altitude. Once the RLV is in close proximity, the TA is expected to glide and get into the formation. The initial altitude and velocity at which this manoeuvre begins can influence the formation time strongly, especially when the aerodynamic performances of both the vehicles are not the same. For instance, if the TA starts the dive at the same altitude, the formation cannot take place because a steep descent beyond the capacity of TA would be required. Therefore, a Monte Carlo study is performed to identify which initial conditions would provide the longest formation times. This study is performed with an initial altitude range between 7500 m to 9000 m and an initial velocity range between 170 m/s and 200 m/s. The RLV is assumed to be non-cooperative at an altitude of 9170 m with a velocity of 197 m/s at the start of the dive.

Fig. 12 shows the effect on formation time for 500 combinations of initial altitude and initial velocity of TA. It can be observed that the longest formations are obtained when the TA dives from a slightly lower altitude between 7500 m and 8500 m. Here a strong correlation with velocity can also be noticed. Diving from higher altitudes work better with lower initial velocities because a lower FPA would be required to match the trajectory. This in turn increases the velocity, which is compensated by starting with a lower initial velocity. However, it is not favourable to start at lower velocities at high altitudes because the flight envelope for commercial aircraft tend to be limited to higher velocities at high altitudes. Therefore, a more affirmative choice would be to select lower altitudes (7500 m – 8000 m) with higher velocities (185 m/s – 200 m/s).

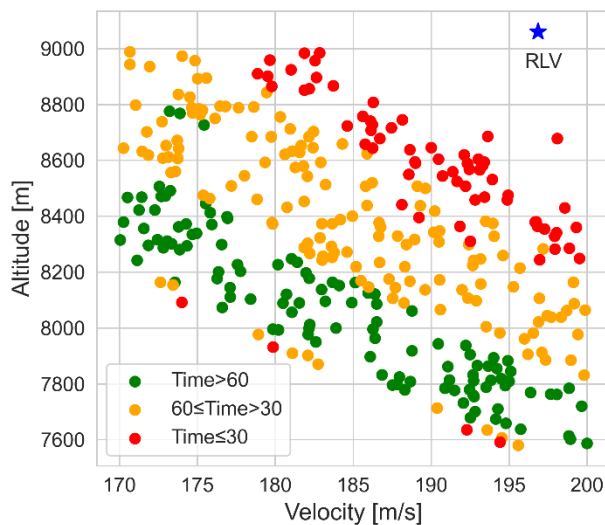


Fig. 12. Sensitivity of Formation Flight Trajectory to the Initial Conditions

1.3 Sensitivity to External Disturbances

During flight, an aircraft is subjected to a number of uncertainties and disturbances originating from technical errors, weather, track changes, signal delays and so on. For the current formation flight scenario, two important external disturbances are identified to be the wake of the aircraft and wind gusts or turbulence during the flight. This section is focussed on examining the sensitivity of formation flight to these disturbances.

1.3.1 Wake Disturbances

As it was marked in Sec. 3.4, the aircraft wake at higher AoAs has a significant downwash component that can disturb the AoA of the RLV when exposed to it. For an AoA of 8°, this component was found to reach up to 11% of free stream velocity. Such a high deficit in vertical velocity can drastically disturb the formation and therefore, should be analysed.

Fig. 13 shows the effect of wake on the AoA of RLV. The time period in which the RLV was exposed to the wake is marked by the orange area, while the green area shows the duration of formation flight. It can be observed from the plot that substantial disturbance has been caused to the RLV AoA at the peak of wake exposure. However, since the exposure to the most perturbing part of the wake is short, the formation was not broken. This can be explained better using Fig. 14, which shows the velocity contour of the wake behind the TA. It can be seen from the figure that the region of highest velocity deficit is limited to a span of about 10 m. Since the RLV simply passes through it, the exposure is not prolonged and AoA is recovered to around 8° as shown in Fig. 13.

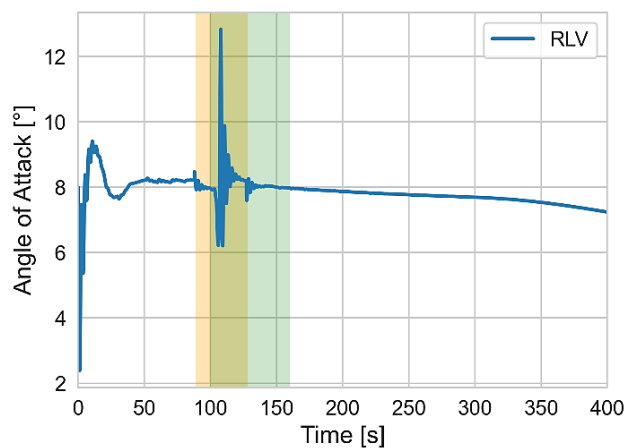


Fig. 13. Sensitivity of RLV AoA and Formation Flight Trajectory to TA Wake

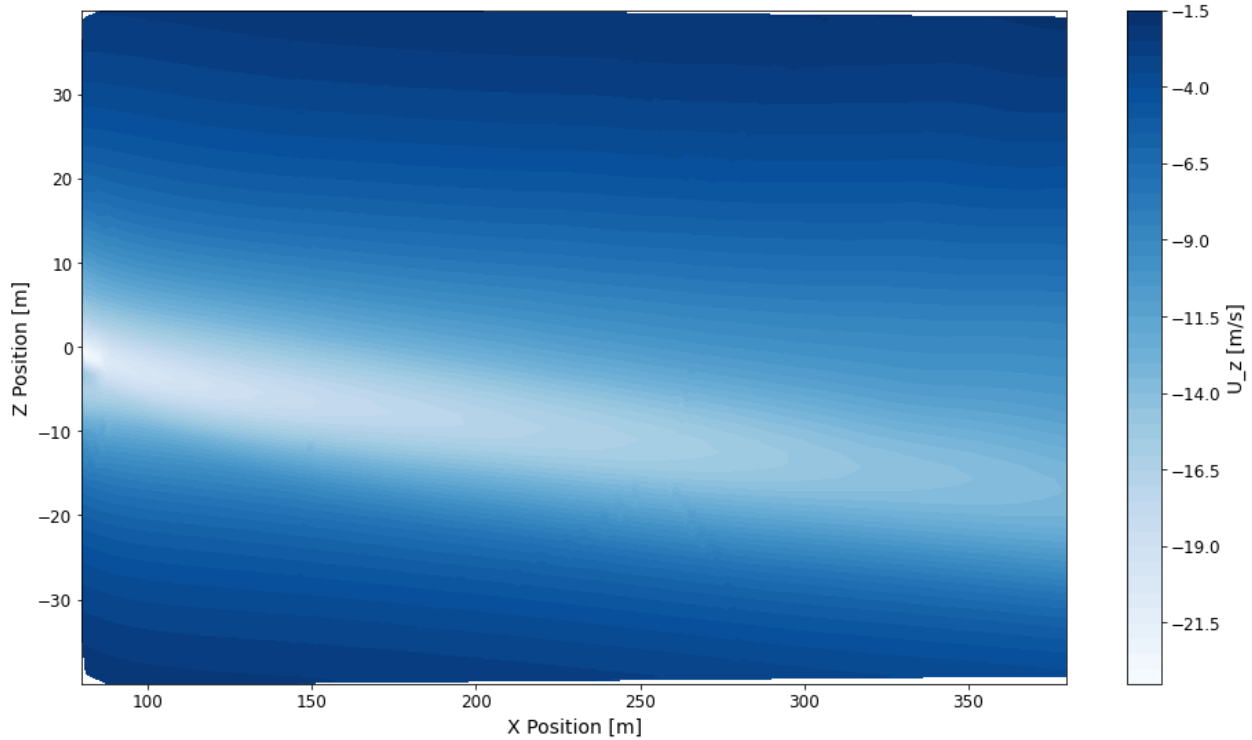


Fig. 14. Wake Velocity Contour in the XZ-Plane

On comparing the formation time in Fig. 13 with the time in Fig. 10(b), it can be concluded that even though the formation is maintained with the wake, the overall duration of formation flight is reduced because of the wake disturbance. Nonetheless, the minimum requirement of 60 s of formation could still be maintained.

1.3.2 Wind Gusts

Wind gusts during formation flight could be challenging since both the vehicles are exposed to it and are affected differently. Large wind gusts can therefore strongly disturb the formation. The average wind velocity ranges between 10 m/s to 20 m/s for an altitude between 3000 m and 8000 m [17]. Since the current simulation is in 3DOF, only the effect of headwind is included. Hence, to analyse the effect of wind as well as wind gusts, a constant wind of 15 m/s is assumed throughout the trajectory with wind gusts of up to 50 m/s applied during the formation flight (indicated by orange area in Fig. 15). More detailed wind models will be included in future work.

It is clear from Fig. 15 that major disturbances are caused in the AoA of both vehicles due to the wind gusts during the formation. However, both vehicles regain stability quickly and are able to maintain the formation. The minimum requirement of a 60 s formation was also met, despite the perturbations (shown in green in Fig. 15).

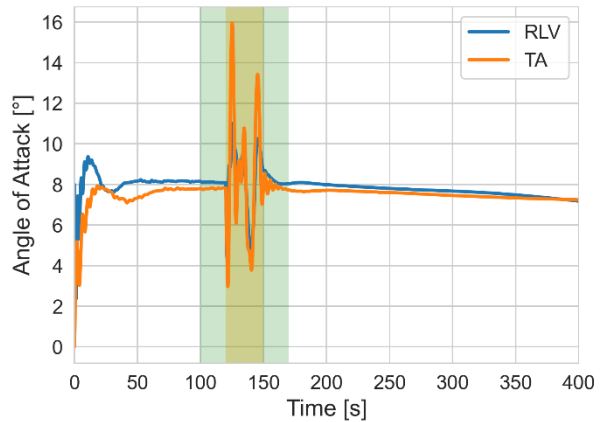


Fig. 15. Sensitivity of TA and RLV AoA to Wind Gusts during Formation Flight.

5. Conclusions and Future Work

A detailed investigation of formation flight in IAC is fundamental to understand the challenges and risks involved in the manoeuvre. This study is aimed at examining this phase through simulation and analysis of full-scale test cases. For this research, the two test vehicles were chosen to be RLVC4-IIIB, which is a large winged stage weighing approximately 80 tons and the A340-600, which is a retired long-range aircraft that can support the towing loads from the large stage. Since the formation flight requires both vehicles to have a similar

velocity, altitude and FPA, their aerodynamic performances should also be similar. Therefore, a comparative study for different TA configurations was performed and it was found that the A340-600 configuration with spoilers deflected to -20° , and with front and main landing gear deployed is the most favourable option for the capture of RLVC4-IIIB.

Next, the role of important subsystems like aerodynamics, propulsion and external disturbances were analysed. RANS studies performed for the selected test cases concluded that the RLV had a maximum L/D ratio of 5.5, while the TA reaches a L/D ratio of 8 at the same AoA of 8° . A simplified model for airbreathing propulsion of TA was included by writing thrust as a function of sea-level thrust, throttle and air density, which changes with altitude. The role of idle thrust in jet engines was also examined and it was deduced that idle thrust (minimum throttle setting) increases the achievable FPA of TA, therefore preventing it from diving too steep. This would further make the formation flight more challenging. Next, the effect of TA mass on its aerodynamics was analysed and it was concluded that larger masses facilitate larger AoAs, which may be required during the dive. Thus, a mass of 280 tons was found suitable for the formation flight simulations. Lastly, RANS studies performed on wake showed that at higher AoAs, the vertical component of the wake could cause considerable disturbance. At the AoA of 6° , the downwash component of the wake amounted to 8% of free stream velocity even at a distance of 200 m from the aircraft.

With the preliminary requirement of maintaining at least 60 s of formation flight, trajectory simulations were performed. The criteria for successful formation required the two vehicles to have a relative distance less than 350 m and the relative velocity within ± 3.5 m/s. From the trajectory simulations, it was found that the required 60 s formation could not be maintained when idle thrust was included. However, without idle thrust, a formation of up to 72 s could be achieved. A monte carlo study performed with different initial velocities and altitudes, indicated that the duration of formation flight is also highly dependent on the initial conditions. Finally, a sensitivity study to analyse the effect of external disturbances showed that the formation could be maintained despite significant disturbances from wake of the TA and wind.

Future work will aim at performing the formation trajectory simulations in 6DOF. Effect of additional factors like sensor fusion, signal delay, noise and so on will also be included. Controlled simulations of the capturing device performing a rendezvous manoeuvre with the RLV with disturbances cause due to the wake and the rope dynamics is also interesting for future studies. Finally, optimized trajectories as previously analysed in [18] and multiple failure scenarios must also be studied for IAC.

Acknowledgements

This work was performed under the Horizon 2020 project ‘Formation flight for in-Air Launcher 1st stage Capturing demonstration’ (FALCon) aimed at development and testing of the ‘In-Air Capturing’ technology. FALCon, coordinated by DLR-SART, is supported by the EU within the Programme 5.iii. Leadership in Enabling and Industrial Technologies – Space with EC grant 821953. Further information on FALCon can be found at <http://www.FALCon-iac.eu>

References

- [1] M. Sippel, J. Klevanski, Simulation of Dynamic Control Environments of the In-Air-Capturing Mechanism, 6th International Symposium on Launcher Technology, 2005.
- [2] Patentschrift (patent specification) DE 101 47 144 C1, Verfahren zum Bergen einer Stufe eines mehrstufigen Raumtransportsystems, released 2003.
- [3] S. Stappert, J. Wilken, L. Bussler, M. Sippel, A Systematic Assessment and Comparison of Reusable First Stage Return Options, IAC-19-D2.3.10, 70th International Astronautical Congress, 2019, 21-25 October.
- [4] M. Sippel, S. Stappert, L. Bussler, S. Krause, S. Cain, J. Espuch, S. Buckingham, V. Penev, Highly Efficient RLV-Return Mode ‘In-Air-Capturing’ Progressing by Preparation of Subscale Flight Tests, 8th European Conference for Aeronautics and Space Sciences (EUCASS), 2019, 1-4 July.
- [5] E. J. Saltzman, Aerodynamic Assessment of Flight-Determined Subsonic Lift and Drag Characteristics of Seven Lifting-body and Wing-body Reentry Vehicle Configurations, National Aeronautics and Space Administration, Dryden Flight Research Center, 2002.
- [6] R. Martinez-Val, E. Perez, J. F. Palacin, Historical Evolution of Air Transport Productivity and Efficiency, AIAA 2005-121, 43rd AIAA Aerospace Sciences Meeting and Exhibit, 2005, 10-13 January.
- [7] M. Sippel, S. Stappert, L. Bussler, C. Messe, Powerful and Flexible Future Launchers in 2-or 3-stage Configuration, IAC-19-D2.4.8, 70th International Astronautical Congress, 2019, 21-25 October.
- [8] A340-600 Global Performer, Previous Generation Aircraft, <https://www.airbus.com/aircraft/previous-generation-aircraft/a340-family/a340-600.html>, (accessed 21.09.2021)

- [9] M. Sippel, S. Stappert, L. Bussler, S. Callsen, High-Performance, Partially Reusable Launchers for Europe, IAC-20-D2.4.1, 71st International Astronautical Congress (IAC), 2020, 12-14 October.
- [10] M. Sippel, S. Stappert, S. Callsen, I. Dietlein, K. Bergmann, A. Gülhan, P. Marquardt, A viable and sustainable European path into space – for cargo and astronauts, IAC-21-D2.4.4, 72nd International Astronautical Congress (IAC), Dubai, 2021, 25-29 October.
- [11] Airbus, Aircraft Characteristics Airport and Maintenance Planning, Airbus SAS France, 2005.
- [12] S. Singh., S. Stappert, S. Buckingham, S. Lopes, Y.C. Kucukosman, M. Simioana, M. Pripasu, A. Wiegand, M. Sippel, P. Planquart, Dynamic Modelling and Control of an Aerodynamically Controlled Capturing Device for ‘In-Air-Capturing’ of a Reusable Launch Vehicle, 11th International ESA Conference on Guidance, Navigation & Control Systems, 2021, 22-25 June.
- [13] European Aviation Safety Agency, EASA Type Certificate Data Sheet, Type: Rolls-Royce plc RB211 Trent 500 Series Engine, 2007, 26 October.
- [14] Federal Aviation Administration, Airplane Flying Handbook FAA-H-8083-3B, 2016.
- [15] P.P. Walsh, P. Fletcher, Gas Turbine Performance, John Wiley & Sons, 2004.
- [16] J.F. Marchman, Introductory Flight Performance, Second Edition, 2001.
- [17] M. Limpinsel, D. Kuo, and A. Vijh, SMARTS Modeling of Solar Spectra at Stratospheric Altitude and Influence on Performance of Selected III-V Solar Cells, IEEE 7th World Conference on Photovoltaic Energy Conversion (WCPEC) (A Joint Conference of 45th IEEE PVSC, 28th PVSEC & 34th EU PVSEC), 2018, 10-15 June.
- [18] L. E. Briese, B. Gäßler, Advanced Modeling and Trajectory Optimization of the In-Air-Capturing Maneuver for Winged RLVs, <https://doi.org/10.1016/j.actaastro.2021.09.005>, Acta Astronautica, 2021.